8536 *Inorg. Chem.* **2009**, *48*, 8536–8543
DOI: 10.1021/ic901303a

Inorganic Chemistry
Article

Sexithiophenes Mediated by MM Quadruple Bonds: MM = Mo_2, MoW, and W_2

Brian G. Alberding, Malcolm H. Chisholm,* Yagnaseni Ghosh, Terry L. Gustafson,* Yao Liu, and Claudia Turro*

Department of Chemistry, The Ohio State University, 100 West 18th Avenue, Columbus, Ohio 43210-1185

Received July 6, 2009

The reactions between MM(TiPB)$_4$, where TiPB = 2,4,6-triisopropylbenzoate and MM = MoW and W_2, and the (2,2′:5′,2″-terthiophene)-5-carboxylic acid, TThH (2 equiv) leads to the formation of new compounds *trans*-MM(TiPB)$_2$(TTh)$_2$, **II** and **III**, respectively, as well as to the previously reported compound **I**, when MM = Mo_2. The compounds have been characterized by elemental analysis, ^{1}H NMR spectroscopy, electronic absorption, and emission spectroscopies together with cyclic voltammetry and differential pulse voltammetry. Calculations on the model compounds **I′**, **II′**, and **III′**, where formate ligands substitute for TiPB, have been carried out employing density functional theory (DFT) and time-dependent DFT. These complexes display intense ^{1}MLCT absorptions (MMδ to thienyl carboxylate) and have oxidations and reductions that are metal (MMδ) and thienyl ligand based, respectively. All compounds show emission in the near-IR region. At low temperature the NIR emission from **I** and **II** shows clear evidence of vibronic features due to υ(MM) $\sim$ 350−390 cm^{-1}, and all compounds show evidence of a vibronic feature due to $\upsilon(CO_2) \sim 1200$ cm^{-1}. Transient absorption spectroscopy reveals relatively short-lived S_1 states, $\tau \sim 10$ ps, and longer lived T_1 states: $\tau \sim 72$ μs for **I**, $\sim$ 160 ns for **II**, and $\sim$ 90 ns for **III**. The chemistry described here reveals the remarkable influence of MMδ to TTh π electronic coupling on the optoelectronic properties of the thienyl chains.

Introduction

Organic conjugated polymers have attracted considerable attention over the past two decades and now find numerous applications in the rapidly emerging field of plastic electronic devices.[1−3] Prime among these materials are oligo- or polythiophenes,[4−7] many of which are sold commercially, for example, P3HT (poly-3-hexyl thiophene) and PEDOT (poly dioxoethylene thiophene). The materials are semiconductors and when doped show good electrical conductivity via hole transport.[8]An attractive feature of these polymers is that chemical modification can be employed so as to enhance their processability and physical properties. For example, the introduction of alkyl groups at 3 and 4 positions enhances solubility,[9−11] and the introduction of electron withdrawing groups can alter the band gap and conductivity.[12,13] So, for example, the introduction of fluoro or fluoroacyl groups can convert a hole transporter to an electron conductor as demonstrated by Marks et al.[14−17] We are interested in the influence of incorporating MM quadruple bonded units (MM = Mo_2, MoW, and W_2) into oligothiophenes by way of carboxylate linkers. The latter allow for both covalent attachments by use of M−O σ bonds and electronic coupling by way of MM δ to thienyl π conjugation.

In general, the introduction of metal ions into conjugated organic π-systems leads to new classes of hybrid organic−inorganic materials.[18,19] The metal atoms may be attached as side-chain appendages or incorporated in the backbone of the polymer.[20] By far the most studied of these systems are those incorporating the group 8 transition metals and the

*To whom correspondence should be addressed. E-mail: chisholm@chemistry.ohio-state.edu (M.H.C.), gustafson@chemistry.ohio-state.edu (T.L.G.), turro@chemistry.ohio-state.edu (C.T.).

(1) Burroughes, J. H.; Bradley, D. D. C.; Brown, A. R.; Marks, R. N.; Mackay, K.; Friend, R. H.; Burns, P. L.; Holmes, A. B. *Nature* **1990**, *347*, 539.
(2) Kraft, A.; Grimsdale, A. C.; Holmes, A. B. *Angew. Chem., Int. Ed.* **1998**, *37*, 403.
(3) *Handbook of Conducting Polymers*, 2nd ed.; Skotheim, T. A.; Elsenbaumer, R. L.; Reynolds, J. R., Eds.; M. Dekker: New York, 1997; p 1112 ff.
(4) Roncali, J. *Chem. Rev.* **1997**, *97*, 173.
(5) McCullough, R. D. *Adv. Mater.* **1998**, *10*, 93.
(6) McQuade, D. T.; Pullen, A. E.; Swager, T. M. *Chem. Rev.* **2000**, *100*, 2537.
(7) Reddinger, J. L.; Reynolds, J. R. *Adv. Polym. Sci.* **1999**, *145*, 57.
(8) Martin, R. E.; Geneste, F.; Holmes, A. B. *C. R. Phys.* **2000**, *1*, 447.
(9) Elsenbaumer, R. L.; Jen, K. Y.; Oboodi, R. *Synth. Met.* **1986**, *15*, 169.
(10) Hotta, S.; Rughooputh, S. D. D. V.; Heeger, A. J.; Wudl, F. *Macromolecules* **1987**, *20*, 212.
(11) Hotta, S.; Soga, M.; Sonoda, N. *Synth. Met.* **1988**, *26*, 267.
(12) Li, L.; Counts, K. E.; Kurosawa, S.; Teja, A. S.; Collard, D. M. *Adv. Mater.* **2004**, *16*, 180.
(13) Pomerantz, M.; Yang, H.; Cheng, Y. *Macromolecules* **1995**, *28*, 5706.
(14) Facchetti, A.; Letizia, J.; Yoon, M.-H.; Mushrush, M.; Katz, H. E.; Marks, T. J. *Chem. Mater.* **2004**, *16*, 4715.
(15) Facchetti, A.; Mushrush, M.; Katz, H. E.; Marks, T. J. *Adv. Mater.* **2003**, *15*, 33.
(16) Facchetti, A.; Yoon, M.-H.; Stern, C. L.; Katz, H. E.; Marks, T. J. *Angew. Chem., Int. Ed.* **2003**, *42*, 3900.
(17) Letizia, J. A.; Facchetti, A.; Stern, C. L.; Ratner, M. A.; Marks, T. J. *J. Am. Chem. Soc.* **2005**, *127*, 13476.
(18) Holliday, B. J.; Swager, T. M. *Chem. Commun.* **2005**, 23.
(19) Pickup, P. G. *J. Mater. Chem.* **1999**, *9*, 1641.
(20) Wolf, M. O. *Adv. Mater.* **2001**, *13*, 545.

 Published on Web 08/12/2009

Scheme 1. Synthesis of $MM(TiPB)_2(TTh)_2$ Complexes; MM = Mo_2, MoW, and W_2

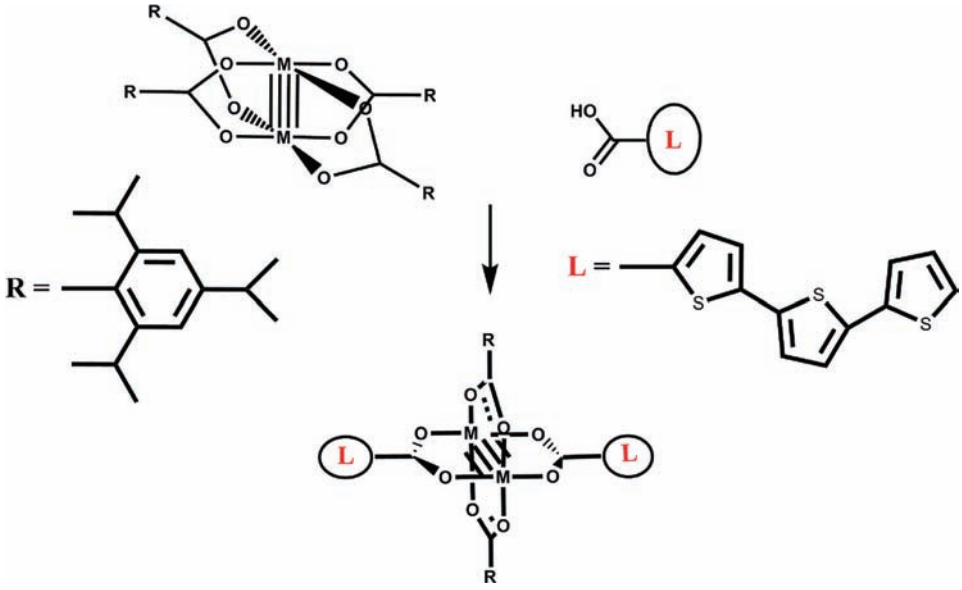

coinage metals as exemplified by the work of Wolf,[21−23] Raithby[24,25] and Wong.[26,27] These assemblies have attracted great attention because of their luminescent properties and their potential applications in various opto-electronic devices and fluorescent detectors. The emission from these complexes is from LLCT or MLCT. To our knowledge triplet emission from a metal centered state, ^{3}MC, has not been observed in this application. We recently reported the synthesis and electronic and photophysical properties of thienyl ligated quadruply bonded dimolybdenum compounds, including the compound, $Mo_2(TiPB)_2(TTh)_2$ (**I**), where, TiPB = 2,4,6-triisopropylbenzoate and TTh = (2,2′:5′,2″-terthiophene)-5-carboxylate, that showed dual emission, namely, a ^{1}MLCT fluorescence and ^{3}MC phosphorescence.[29] In this paper we describe the synthesis and properties of a series of compounds, $MM(TiPB)_2(TTh)_2$, of the structural type shown in Scheme 1 where the dinuclear MM center is MoW and W_2 and compare them with the related compound **I**, where MM is Mo_2. These compounds show remarkable properties that arise from the electronic coupling of the MMδ and thienyl carboxylate π-systems and in many ways are quite different from those of earlier studies of metalated oligothiophenes. They are model compounds for oligothiophenes incorporating these MM units which are currently under study in this laboratory.

Results and Discussion

Synthesis. The general method for the preparation of **II** and **III**, as well as the previously described compound, **I**,[29] is outlined in Scheme 1. Reactions carried out in toluene proceed with a marked color change and the precipitation of the products.

All three compounds are air-sensitive and appreciably soluble in THF and other donor solvents but less soluble in simple hydrocarbon solvents such as hexane and toluene. The compounds show molecular ions ($\mathbf{I}^+$, $\mathbf{II}^+$, $\mathbf{III}^+$) by matrix assisted laser desorption/ionization time-of-flight (MALDI-TOF) and they gave satisfactory elemental analyses.

The ^{1}H NMR data are consistent with the trans-substitution pattern at the MM center and ^{1}H NMR data are given in the Experimental Section. Previous studies have also confirmed the trans geometry in the compounds $Mo_2(TiPB)_2(Th)_2$[28] and $Mo_2(TiPB)_2(BTh)_2$[29] where Th is thiophene-5-carboxylic acid and BTh is 2,2′-bithiophene-5-carboxylic acid. In these structures the thienyl rings are also essentially coplanar with the carboxylate CO_2 moieties as was also seen in the compound *trans*-$W_2(TiPB)_2(Azu)_2$,[30] where Azu = 2-carboxy-6-ethoxyazulene. As we show later in the calculations, *vide infra*, this planar trans-geometry favors and maximizes thienyl carboxylate-MMδ-thienyl carboxylate interactions.

Electrochemical Studies. The compounds **I**, **II**, and **III** show reversible one electron oxidation waves by cyclic voltammetry and differential-pulse voltammetry that are readily assignable to the reversible oxidation of the MM center. The oxidation potentials reveal the ease of removal of an electron from the MMδ orbital, and the potentials are essentially identical to those of the parent $MM(TiPB)_4$ compounds.[31] There is roughly 0.5 V difference between the $Mo_2^{4+/5+}$ and the $W_2^{4+/5+}$couple.

(21) Wolf, M. O.; Patrick, B. O.; Stott, T. L. *Can. J. Chem.* **2007**, *85*, 383.
(22) Moorlag, C.; Sih, B. C.; Stott, T. L.; Wolf, M. O. *J. Mater. Chem.* **2005**, *15*, 2433.
(23) Moorlag, C.; Clot, O.; Wolf, M. O. *Polym. Prepr.—Am. Chem. Soc., Div. Polym. Chem.* **2004**, *45*, 437.
(24) Li, P.; Ahrens, B.; Feeder, N.; Raithby, P. R.; Teat, S. J.; Khan, M. S. *Dalton Trans.* **2005**, 874.
(25) Chawdhury, N.; Kohler, A.; Friend, R. H.; Wong, W. Y.; Lewis, J.; Younus, M.; Raithby, P. R.; Corcoran, T. C.; Al-Mandhary, M. R. A.; Khan, M. S. *J. Chem. Phys.* **1999**, *110*, 4963.
(26) Wong, W.-Y.; Wang, X.-Z.; He, Z.; Chan, K.-K.; Djurisic, A. B.; Cheung, K.-Y.; Yip, C.-T.; Ng, A. M.-C.; Xi, Y. Y.; Mak, C. S. K.; Chan, W.-K. *J. Am. Chem. Soc.* **2007**, *129*, 14372.
(27) Wong, W.-Y.; Zhou, G.-J.; He, Z.; Cheung, K.-Y.; Ng, A. M.-C.; Djurisic, A. B.; Chan, W.-K. *Macromol. Chem. Phys.* **2008**, *209*, 1319.
(28) Chisholm, M. H.; Epstein, A. J.; Gallucci, J. C.; Feil, F.; Pirkle, W. *Angew. Chem., Int. Ed.* **2005**, *44*, 6537.
(29) Burdzinski, G. T.; Chisholm, M. H.; Chou, P. T.; Chou, Y. H.; Feil, F.; Gallucci, J. C.; Ghosh, Y.; Gustafson, T. L.; Ho, M. L.; Liu, Y.; Ramnauth, R.; Turro, C. *Proc. Natl. Acad. Sci.* **2008**, *105*, 15247.
(30) Barybin, M. V.; Chisholm, M. H.; Patmore, N. J.; Robinson, R. E.; Singh, N. *Chem. Commun.* **2007**, 3652.
(31) Alberding, B. G.; Chisholm, M. H.; Chou, Y.-H.; Gallucci, J. C.; Ghosh, Y.; Gustafson, T. L.; Patmore, N. J.; Reed, C. R.; Turro, C., *Inorg. Chem.* **2009**, *48*, 4394.

Scheme 2. Orbital Interaction between M_2 δ and $-CO_2$ π^* Orbitals in a $M_2(TiPB)_2(O_2C\text{-}L)_2$ Type Compound[a]

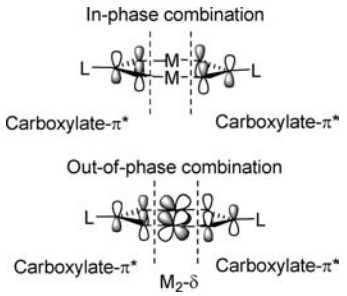

[a] L = conjugated organic ligand.

The compounds also show reduction waves that are not reversible but can be readily assigned to being associated with the complexes, that is, not solvent based reductions. What is most interesting is that the first reduction wave shows clear evidence of having two components in going from **I** to **II** to **III**. Given the higher energy of the MMδ orbital with increasing W content in the MM core this is consistent with the formation of ligand centered radicals, $\mathbf{I}^-$, $\mathbf{II}^-$, and $\mathbf{III}^-$ that may be classified as Class II or III on the Robin and Day Scheme.[32] This arises because of the coupling of the out-of-phase π^*-thienyl carboxylate orbitals with the MMδ as shown in Scheme 2.

The differential pulse voltammograms of the three compounds are compared in Figure 1, and details are reported in the Experimental Section.

Electronic Absorption Spectra. The absorption spectra of compounds **I**, **II**, and **III** in tetrahydrofuran (THF) are shown in Figure 2. The intense broad absorptions bands in the visible region of the spectrum arise from ^{1}MLCT (MMδ to thienyl carboxylate π^*). With the change from MM = Mo_2 to MoW to W_2, we observe the systematic red shift which correlates with the equivalent rise in energy of the MMδ orbitals as noted above in the electrochemical studies. At higher energy and $\lambda_{max} \sim 380$ nm, there is for each compound an intense absorption that we assign to a thienylcarboxylate ^{1}LC transition. This absorption is similar to that of the free acid, TTh-H (see the Supporting Information, Figure S1).Whereas the molar absorptivity of ^{1}LC transition remains virtually constant, we note that the ^{1}MLCT for MM = W_2 is significantly more intense than for MM = Mo_2. A similar trend has been seen before in related compounds and correlates with the general "rule of thumb" that the intensity of an MLCT transition is inversely proportional to the energy separation of the two states and correlates with orbital overlap. However, as can be seen in Figure 2, the relative intensity of the ^{1}MLCT for the MoW containing complex does not appear to follow this trend, though a quantitative measure of this is not easy to judge since the separation of the ^{1}LC and ^{1}MLCT absorptions are much greater for compound **II** relative to compound **I**. Moreover in compound **I**, there is likely a contribution from the tail of the ^{1}LC absorption to the intensity of the ^{1}MLCT absorption.

Luminescence Studies. The compounds **I**, **II**, and **III** all show room temperature emission in the near-infrared (NIR) (950−1300 nm) as shown in Figure 3 *Top*. With excitation at 532 nm for MM = Mo_2 and at 658 nm for

(32) Robin, M. B.; Day, P. *Adv. Inorg. Chem. Radiochem.* **1967**, *10*, 247.

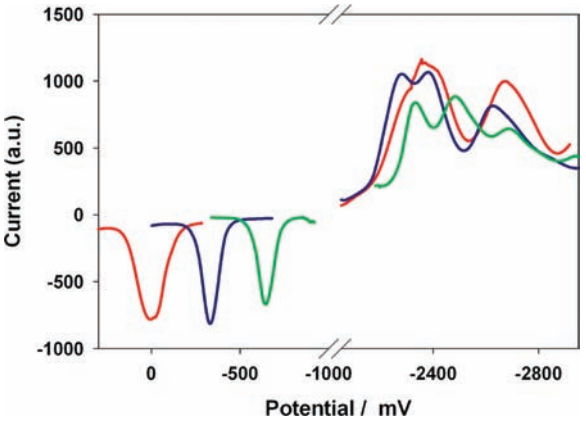

Figure 1. Differential pulse voltammograms for the compounds MM-$(TiPB)_2(TTh)_2$ where, MM = Mo_2 (**I**) in red; MM = MoW (**II**) in blue and MM = W_2 (**III**) in green, showing the metal based oxidation of the MMδ orbital and the thienyl carboxylate reductions. The potentials are referenced to the $Cp_2Fe^{0/+}$ couple.

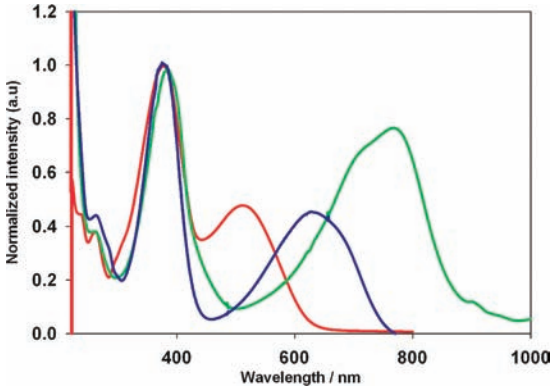

Figure 2. Absorption spectra for the compounds $MM(TiPB)_2(TTh)_2$ where, MM = Mo_2 (**I**) in red; MM = MoW (**II**) in blue and MM = W_2 (**III**) in green in THF at room temperature.

MM = MoW and W_2, we note that the emission is significantly weaker for the MoW containing compound. We should also note that compound **I** shows emission at ~700 nm at room temperature which we have previously assigned to fluorescence from the ^{1}MLCT state.[29] No such emission in the visible region is observed for compounds **II** and **III**. It should be mentioned here that the emission from the pure TTh-H acid occurs at a much higher energy (see Supporting Information, Figure S1), and it can therefore be assumed that the NIR emission from these compounds arises not from any free ligand impurity.

The low temperature emission spectra obtained from frozen glasses in 2-MeTHF at 77 K are shown in Figure 3, *Bottom*. Compound **I** shows clear evidence of vibronic features associated with υ(MoMo) ~ 390 cm^{-1}. The compound **II**, which shows weaker emission, does show vibronic features at 77 K, and an estimate of vibrational spacing is ~330 cm^{-1} which may be assigned to υ(MoW).

The emission spectrum of the W_2-containing complex at 77 K does not show vibronic features due to υ(WW) but rather an ill-resolved vibronic feature with a spacing of ~1200 cm^{-1}. A closer inspection of the spectra obtained for **I** and **II** also reveals evidence of vibronic features to lower energy with $\upsilon \sim 1200$ cm^{-1}. This we suggest arises

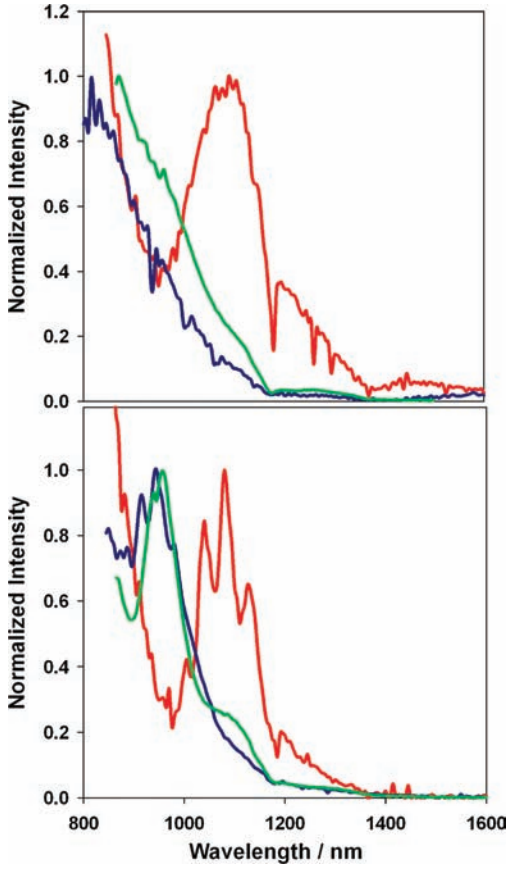

Figure 3. NIR emission spectra for $MM(TiPB)_2(TTh)_2$ compounds, where MM = Mo_2 (red), = MoW (blue), and = W_2 (green). *Top*: Room temperature in THF, *Bottom*: 77 K in 2-MeTHF.

from a υ(thienyl carboxylate) mode. A similar ligand-based progression is observed for $Ru(bpy)_3^{2+}$ at 77 K.[33]

Whereas, the NIR emission of compound **I** does not show solvatochromism, we do observe solvatochromism for the NIR emission of compounds **II** and **III**, on changing the solvent from THF to DMSO (see Supporting Information, Figure S2). Consequently, we suggest that on the basis of the small Stokes shift from the ^{1}MLCT absorption band and the solvatochromism, the NIR emission of **II** and **III** corresponds to emission from the ^{1}MLCT excited state, while for compound **I** the NIR emission arises from the ^{3}MM$\delta\delta$* state. Further corroboration of our assignments comes from the nanosecond (ns) and femtosecond (fs) transient absorption (TA) measurements which are discussed in the following section.

Transient Absorption Spectroscopy. Femtosecond TA spectra were obtained upon excitation of the compounds **II** and **III** at 675 nm. The TA spectra and the corresponding lifetimes obtained by kinetic traces are shown in Figure 4. An examination of TA spectra indicates the similarity observed between the two compounds. Both show an initial intense absorption in the low energy region of the spectra (500−630 nm) as well as higher energy bleach (380−400 nm) corresponding to the ground state ^{1}LC absorption. The initial intense absorption decays and directly gives rise to the board absorption in the 400−550 nm range, which is consistent with the presence of the reduced or quinoid form of the TTh-H ligand.[34] Furthermore, this band is also comparable to that observed for the ^{3}MLCT state observed in the ns TA experiment, *vide infra*. The lifetimes of the initial excited states obtained by fs TA were found to be ~4 ps for **II** and ~ 20 ps for **III** which can be assigned as ^{1}MLCT. This ^{1}MLCT excited state decays by fluorescence in the NIR region. Furthermore the NIR emission of **III** has a lifetime < 10 ns, which is consistent with the fs TA measurements. Regrettably for **II** low luminescence quantum efficiency made determination of its emission lifetime impossible. It should also be noted in Figure 4 that the bleach signals of **II** and **III** are still evident at 12.5 ps and 100 ps, respectively, indicating that the complexes have not yet returned to the ground state.

To investigate longer-lived excited states, ns TA measurements were also carried out on these compounds. Upon excitation of **II** and **III** at 532 nm, it was found that the TA signals decayed monoexponentially with lifetimes of τ = 165 ns for MM = MoW and τ ~ 90 ns for MM = W_2. Previous studies found a state with τ = 72 μs for MM = Mo_2 upon excitation at 532 nm.[29] Upon examination of the ns TA spectra for the compounds **II** and **III** shown in Figure 5, similarities are again observed between the two. Both complexes show bleaching in > 400 nm region (^{1}LC) and positive, intense absorption features are observed at lower energies, from 400 to 800 nm range. The spectral differences between the compounds are the contribution from the bleaching for **II** at ~630 nm and for **III** at > 700 nm. Such a similarity in the TA signals of **II** and **III** point to their origin from very similar excited states. The broad, intense absorption throughout the visible region is consistent with that arising from a reduced TTh-H ligand (TTh^-), and therefore the states giving rise to the signal are assigned to the ^{3}MLCT excited states for these two compounds. The spectral properties resemble that published for a related terthiophene complex of Ru(II), with strong ^{3}MLCT absorption from 400 to 800 nm.[35] It can be reasonably assumed that these ^{3}MLCT excited states are very low lying in energy, by virtue of the highly delocalized TTh ligands making their deactivation primarily non-radiative. This hypothesis is consistent with the lack of low energy triplet emission for compounds **II** and **III**. In contrast, for compound **I**, the longer lived triplet excited state is assigned to be a ^{3}MM$\delta\delta$* state, which decays by phosphorescence in the NIR region at ~1100 nm.

As previously observed and shown in the Supporting Information, Figure S3,[29] the ns TA of **I** exhibits bleaching at < 380 nm and at ~520 nm, consistent with its ground state absorptions. Positive absorption is observed with a maximum at ~420 nm; however, no transient signal is apparent from 600 to 800 nm. The strong absorption of the ^{3}MLCT of **II** and **III** are at λ > 720 nm and at 600−700 nm, respectively. The strong TA signal throughout the visible and NIR is typical of MLCT excited states involving reduced organic ligands. The absence of this broad absorption in the Mo_2-complex, **I**,

(33) Thompson, D. W.; Schoonover, J. R.; Graff, D. K.; Fleming, C. N.; Meyer, T. J. *J. Photochem. Photobiol., A* **2000**, *137*, 131.

(34) Pappenfus, T. M.; Raff, J. D.; Hukkanen, E. J.; Burney, J. R.; Casado, J.; Drew, S. M.; Miller, L. L.; Mann, K. R. *J. Org. Chem.* **2002**, *67*, 6015.

(35) Barbieri, A.; Ventura, B.; Flamigni, L.; Barigelletti, F.; Fuhrmann, G.; Baeuerle, P.; Goeb, S.; Ziessel, R. *Inorg. Chem.* **2005**, *44*, 8033.

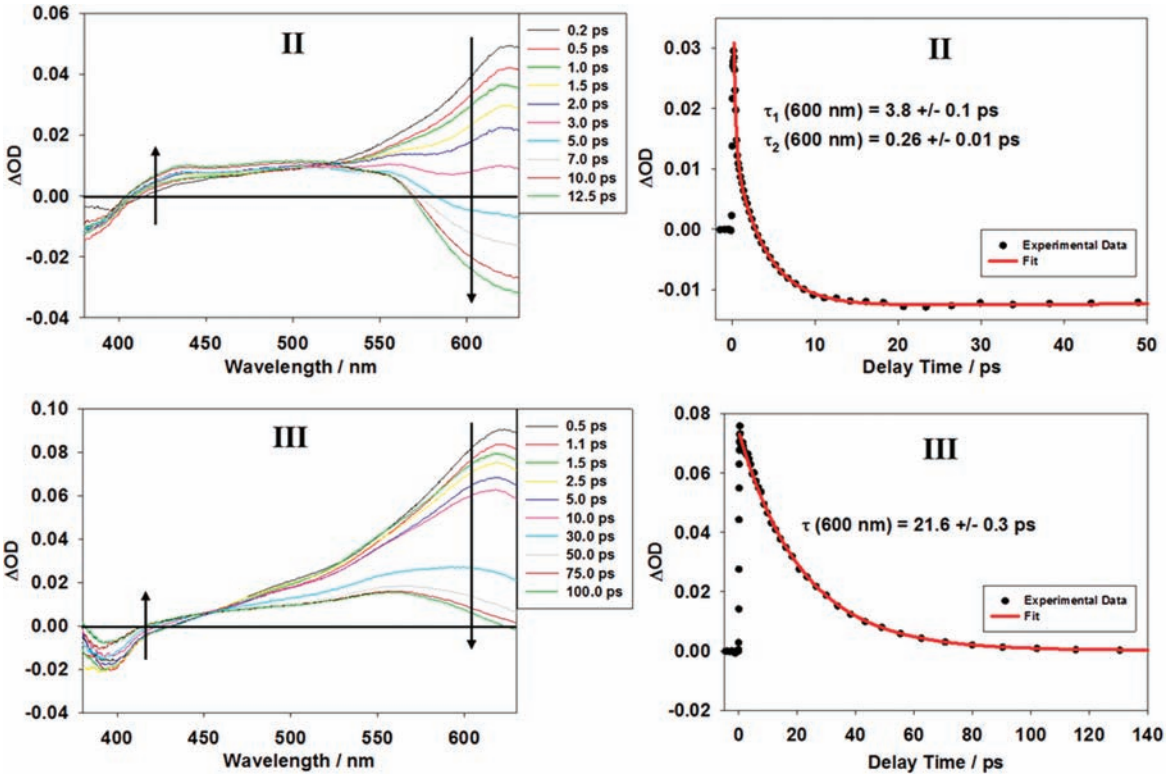

Figure 4. Femtosecond TA spectra for compounds $MoW(TiPB)_2(TTh)_2$ (**II**) and $W_2(TiPB)_2(TTh)_2$ (**III**) in THF excited at 675 nm. Right: Representative kinetics for the singlet state decay.

is consistent with the assignment of the long-lived transient as $^3MM\delta\delta^*$.

Overall, it is seen, that when the dinuclear core has MM = MoW and W_2, the emissive properties and lifetimes of the excited states are very different compared to that for MM = Mo_2, even when the same ligand, TTh, is used. This is in sharp contrast to our observations on the emissive properties of the compounds $MM(TiPB)_4$, where it was found that the singlet and triplet excited states for all three compounds were the same, namely, ^{1}MLCT and $^3MM\delta\delta^*$ states, respectively.[31]

Thus we see that with increasing π-delocalization in the ligand, for example, TTh, the nature of the triplet excited state changes from MM based in Mo_2 to M−L based in MoW and W_2. This is because with the heavier elements, there is greater overlap between the MM δ orbitals and TTh π^* orbitals, causing greater stabilization of the ^{3}MLCT states. The $^3MM\delta\delta^*$ state in compounds **II** and **III** exists but at a higher energy. The lowering of the energy of the ^{3}MLCT states in **II** and **III** is so pronounced that the deactivation occurs via a non-radiative route, which can be explained by the energy gap law.[36−42]

Electronic Structure Calculations. Calculations were carried out on the model compounds *trans*-$MM(O_2CH)_2(TTh)_2$ where MM = Mo_2 (**I′**), MoW (**II′**), and W_2 (**III′**) by employing density functional theory (DFT)[43−46] as implemented in Gaussian 03 suite of programs,[47] and the frontier orbital energy level diagrams for these three molecules are shown in Figure 6. Gaussview[48] plots for the ditungsten compound are shown in Figure 7. In all cases the highest occupied molecular orbital (HOMO) was the MMδ orbital with very little mixing with the terthienyl carboxylate ligand. In going from Mo_2 to MoW to W_2 there is a steady increase in orbital energy of the MMδ as expected based on the redox chemistry.

(36) Avouris, P.; Gelbart, W. M.; El-Sayed, M. A. *Chem. Rev.* **1977**, *77*, 793.
(37) *Radiationless Processes in Molecules and Condensed Phases*; Fong, F. K., Ed.; Springer Verlag: Berlin, 1976; Topics in Applied Physics, Vol. *15*, p 360 ff.
(38) Freed, K. F. *Acc. Chem. Res.* **1978**, *11*, 74.
(39) Heller, E. J.; Brown, R. C. *J. Chem. Phys.* **1983**, *79*, 3336.
(40) Henry, B. R.; Siebrand, W. *Org. Mol. Photophys.* **1973**, *1*, 153.
(41) *Excited States*; Lim, E. C., Ed., Academic Press: New York, 1979; Vol. *4*, p 400 ff.
(42) *Radiationless Transitions*; Lin, S. H., Ed.; Academic Press: New York, 1980; p 425 ff.
(43) Hohenberg, P.; Kohn, W. *Phys. Rev.* **1964**, 164.
(44) Kohn, W.; Sham, L. J. *Phys. Rev.* **1965**, *137*, 1697.
(45) Parr, R. G.; Yang, W. *Density-functional Theory of Atoms and Molecules*; Oxford University Press: New York, 1989; p 333.
(46) Salahub, D. R.; Zerner, M. C., Eds.; *ACS Symposium Series 394: The Challenge of d and f Electrons: Theory and Computation. Developed from a Symposium at the 3rd Chemical Congress of North America Toronto, Can., June 5−11, 1988*. 1989; p 405.
(47) Frisch, M. J. T., G. W.; Schlegel, H. B.; Scuseria, G. E.; Robb, M. A.; Cheeseman, J. R.; Montgomery, Jr., J. A.; Vreven, T.; Kudin, K. N.; Burant, J. C.; Millam, J. M.; Iyengar, S. S.; Tomasi, J.; Barone, V.; Mennucci, B.; Cossi, M.; Scalmani, G.; Rega, N.; Petersson, G. A.; Nakatsuji, H.; Hada, M.; Ehara, M.; Toyota, K.; Fukuda, R.; Hasegawa, J.; Ishida, M.; Nakajima, T.; Honda, Y.; Kitao, O.; Nakai, H.; Klene, M.; Li, X.; Knox, J. E.; Hratchian, H. P.; Cross, J. B.; Bakken, V.; Adamo, C.; Jaramillo, J.; Gomperts, R.; Stratmann, R. E.; Yazyev, O.; Austin, A. J.; Cammi, R.; Pomelli, C.; Ochterski, J. W.; Ayala, P. Y.; Morokuma, K.; Voth, G. A.; Salvador, P.; Dannenberg, J. J.; Zakrzewski, V. G.; Dapprich, S.; Daniels, A. D.; Strain, M. C.; Farkas, O.; Malick, D. K.; Rabuck, A. D.; Raghavachari, K.; Foresman, J. B.; Ortiz, J. V.; Cui, Q.; Baboul, A. G.; Clifford, S.; Cioslowski, J.; Stefanov, B. B.; Liu, G.; Liashenko, A.; Piskorz, P.; Komaromi, I.; Martin, R. L.; Fox, D. J.; Keith, T.; Al-Laham, M. A.; Peng, C. Y.; Nanayakkara, A.; Challacombe, M.; Gill, P. M. W.; Johnson, B.; Chen, W.; Wong, M. W.; Gonzalez, C.; Pople, J. A. *Gaussian 03*; Gaussian,Inc.: Wallingford, CT, 2004.
(48) Dennington, R. K. T., II; Millam, J.; Eppinnett, K.; Hovell, W. L.; Gilliland, R., 2003.

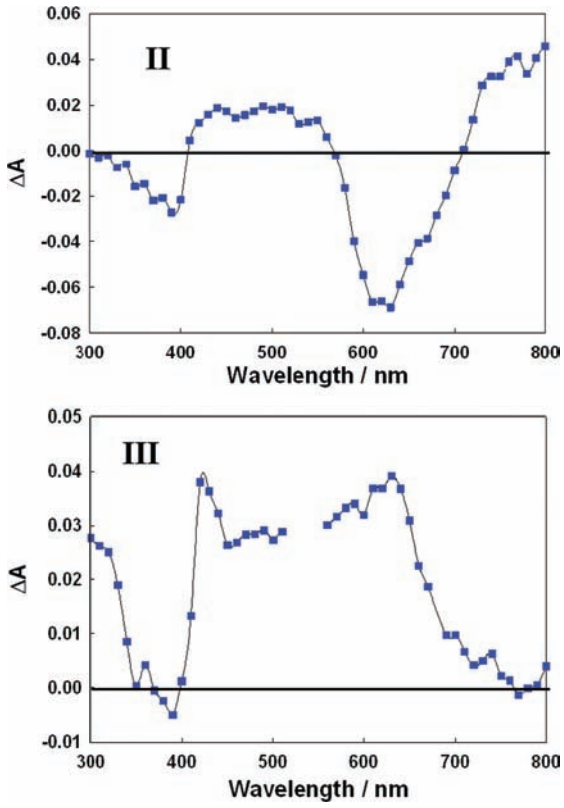

Figure 5. Comparison of ns TA spectra of $MoW(TiPB)_2TTh_2$ (II) and $W_2(TiPB)_2TTh_2$ (III) in THF collected immediately after laser pulse (l_{ex} = 532 nm, fwhm ~8 ns).

In all cases the lowest unoccupied molecular orbital (LUMO) and LUMO +1 are the in-phase and out-of-phase π^* combinations of the terthienylcarboxylate and the energy separation between these orbitals increases along the series Mo_2 < MoW < W_2. The energy separation is due to the mixing with the MMδ (MMδ to ligand π^* back-bonding), and this is greatest for W_2 because of both overlap and energy considerations.

Below the HOMO two thienyl ligand π-based orbitals are calculated, one of which, the HOMO−2, mixes with the $M_2\delta$ orbital. Here the energy separation between the HOMO−1 and HOMO−2 decreases in the order Mo_2 > MoW > W_2 because of the relative energies of the MMδ orbitals.

Above the LUMO and LUMO +1 come the $M_2\delta^*$ metal based orbitals, which have essentially no mixing with any of the ligand orbitals. Below the HOMO −2 are the metal-based MM π orbitals, followed by four sets of ligand filled π orbitals and then the MMσ orbital.

As is evident from the energy level diagram shown in Figure 7, the HOMO−LUMO gap steadily decreases from Mo_2 > MoW > W_2 and is thus consistent with the observed trends in the ^{1}MLCT absorptions shown in Figure 2.

Concluding Remarks

The present series of compounds show significantly different electro-optical properties when compared to other metalated oligothiophenes. The d^8 and d^{10} metal complexes have thienyl ligand and metal based oxidations,[49−52] and their electronic spectra are dominated by π to π^* transitions[25,49,50,53] which are notably higher in energy than the ^{1}MLCT absorptions seen for **I**, **II**, and **III**. Spin orbit coupling from the second and third row metal mixes with these ^{1}LC states so that the emission is seen from both S_1 and T_1 states. The d^6 ferrocenyl and Ru(II) alkynyl linked thienyl derivatives or bipyridyl substituted thienyl derivatives have metal based and thienyl oxidations. The carboxylate linker to the MM^{4+} unit mediates the rate of intersystem crossing such that the ^{1}MLCT is detectable by TA spectroscopy, and for M = Mo, both fluorescence and phosphorescence is seen. However, the emissive metal based T_1 state for molybdenum, ^{3}MoMo$\delta\delta^*$, is most unusual for a transition metal ion since metal based states (ligand field dd states) are dark and decay rapidly.[54] Thus the emissive ^{3}MoMo$\delta\delta^*$ state at ~1100 nm is more reminiscent of a lanthanide ion.[55] With increasing tungsten content the compounds **II** and **III** show only emission from the S_1, ^{1}MLCT state and the triplet MLCT state can only be detected by TA spectroscopy. These states have notably shorter lifetimes than the ^{3}MM$\delta\delta^*$ state and their photophysical properties are collectively summarized in the Jablonski diagram shown in Figure 8.

Finally, the ability to tune the MMδ orbital energy within the series MM = Mo_2, MoW, and W_2 allows the electronic absorptions to traverse the entire region of the spectrum from the UV to the NIR, and this is a property that we seek to employ in photon harvesting devices based on oligothiophenes incorporating MM quadruple bonds.

Experimental Section

Measurements. NMR spectra were recorded on a 400 MHz Bruker DPX Advance400 spectrometer. All ^{1}H NMR chemical shifts are in ppm relative to the protio impurity in THF-d_8 at 3.58 ppm.

Electronic spectra at room temperature were recorded using a Perkin-Elmer Lambda 900 spectrometer in THF solution. A 10.00 mm IR quartz cell was employed.

The cyclic voltammogram (scan rate of 100 mV s^{-1}) and differential pulse voltammogram of all the complexes were collected, using a Princeton Applied Research (PAR) 173A potentiostat-galvanostat equipped with a PAR 176 current-to voltage converter. Electrochemical measurements were performed under an inert atmosphere in a 0.5 M solution of $^nBu_4NPF_6$ in THF inside a single compartment voltammetric cell equipped with a platinum working electrode, a platinum wire auxiliary electrode, and a pseudoreference electrode consisting of a silver wire in 0.5 M $^nBu_4NPF_6$/THF separated from the bulk solution by a Vycor tip. The potential values are referenced to the $FeCp_2/FeCp_2^+$ couple, obtained by addition of a small amount of $FeCp_2$ to the solution.

Nanosecond TA measurements were carried out in 1 × 1 cm square quartz cuvettes equipped with Kontes stopcocks. Nanosecond TA spectra were measured on a home-built instrument pumped by a frequency doubled (532 nm) or tripled (355 nm) Spectra-Physics GCR-150 Nd:YAG laser (fwhm ~ 8 ns, ~5 mJ per pulse). The signal from the photomultiplier tube

(49) Zhu, Y.; Wolf, M. O. *Chem. Mater.* **1999**, *11*, 2995.
(50) Zhu, Y.; Millet, D. B.; Wolf, M. O.; Rettig, S. J. *Organometallics* **1999**, *18*, 1930.
(51) Moorlag, C.; Wolf, M. O.; Bohne, C.; Patrick, B. O. *J. Am. Chem. Soc.* **2005**, *127*, 6382.
(52) Trouillet, L.; De Nicola, A.; Guillerez, S. *Chem. Mater.* **2000**, *12*, 1611.
(53) Thomas, K. R. J.; Lin, J. T.; Lin, K.-J. *Organometallics* **1999**, *18*, 5285.
(54) Bargawi, K. R.; Llobet, A.; Meyer, T. J. *J. Am. Chem. Soc.* **1988**, *110*, 7751.
(55) Bunzli Jean-Claude, G.; Piguet, C. *Chem Soc Rev* **2005**, *34*, 1048.

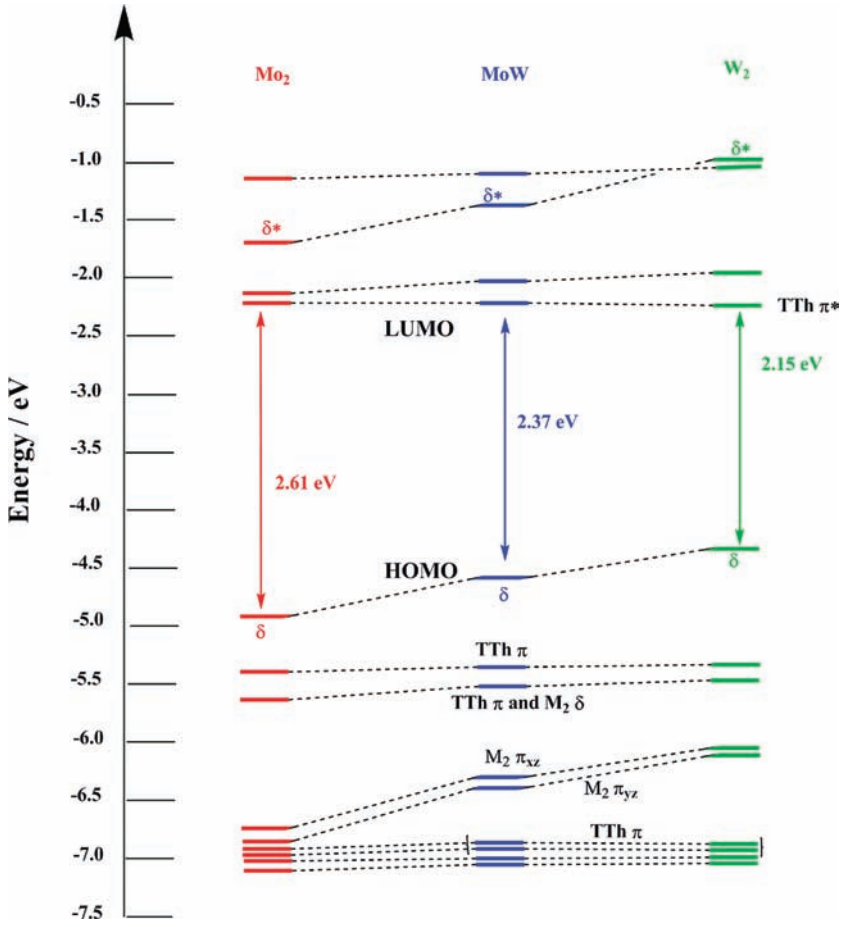

Figure 6. Frontier molecular orbital energy level diagrams for the compounds $MM(O_2CH)_2(TTh)_2$, where MM = Mo_2 (**I′**) in red, MoW (**II′**) in blue, and W_2 (**III′**) in green.

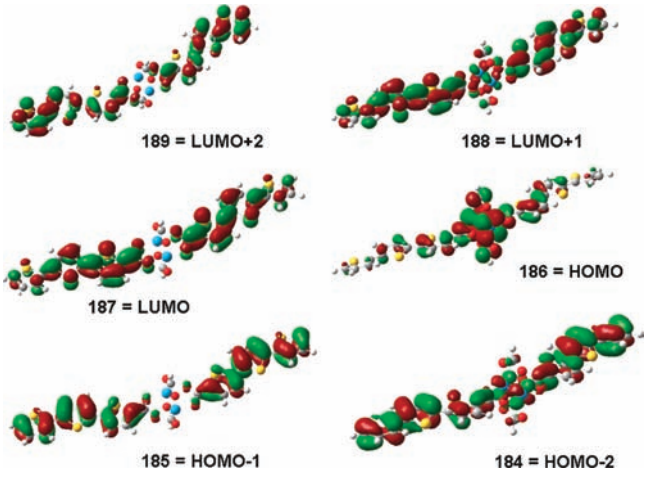

Figure 7. Gaussview plots of the frontier orbitals for the $W_2(O_2CH)_2(TTh)_2$ (**II′**) compound, where the HOMO is 186 and the LUMO 187, drawn at isosurface value of 0.2.

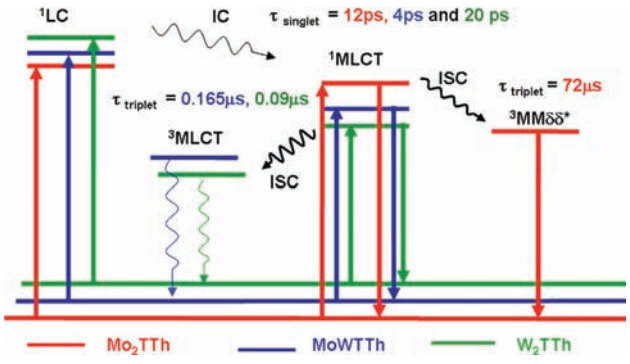

Figure 8. Jablonski diagram depicting the primary excitation and deactivation pathways and the excited state lifetimes for $MM(TiPB)_2(TTh)_2$ compounds, where MM = Mo_2, MoW, and W_2.

(Hamamatsu R928) was processed by a Tektronics 400 MHz oscilloscope (TDS 380).[56]

The steady-state NIR-luminescence measurements at 77 K were carried out in J. Young NMR tubes. The spectra were measured on a home-built instrument utilizing a germanium detector. The sample was excited at 658 nm (laser diode max power: 65 mW) and a RG830 long pass filter was placed between the sample and the detector.

In the femtosecond TA experiments, samples of Mo_2TTh were excited at 365 and 514 nm (second harmonics) or 800 nm of a femtosecond Ti-Sapphire oscillator (82 MHz, Spectra Physics) and monitored with a supercontinuum probe pulse in the spectral range of 500−800 nm. The recorded spectra were time-corrected for the chirp of the supercontinuum. All transient signals were linearly dependent on the excitation power. The time resolution of the system is 300 fs, as determined by the two-photon absorption of methanol in the sample cell. For MoWTTh and W_2TTh, the experiments were carried out

(56) Byrnes, M. J.; Chisholm, M. H.; Gallucci, J. A.; Liu, Y.; Ramnauth, R.; Turro, C. *J. Am. Chem. Soc.* **2005**, *127*, 17343.

using a different laser and detection system, which have been previously described.[57] The samples were excited at 675 nm (with excitation power ~1−2 μJ at the sample) and were prepared with absorbance ~0.4−0.8 at the excitation wavelength. During the measurements, the samples were kept in constant motion by manual movement of an *XYZ* stage in the vertical and horizontal directions. In order ensure that no photodecomposition occurred during data collection, absorption spectra were recorded before and after the TA measurements. The measurements were repeated five times at each of the pump−probe delay positions to confirm data reproducibility throughout the experiment and the resulting spectra were corrected for the chirp in the white-light super continuum. The kinetics were fit to a single exponential decay of the form, $S(t) = A\exp(-t/\tau) + C$, with amplitude, A, lifetime, τ, and offset, C, using SigmaPlot 10.0. Error bars for the lifetimes are reported as the standard error of the exponential fit.

Microanalysis was performed by H. Kolbe Microanalytisches Laboratorium, Germany. MALDI-TOF was performed on a Bruker Reflex III (Bruker, Bremen, Germany) mass spectrometer operated in a linear, positive ion mode with an N_2 laser. Dithranol was used as the matrix and prepared as a saturated solution in THF. Allotments of matrix and sample were thoroughly mixed together; 0.5 mL of this was spotted on the target plate and allowed to dry.

Synthesis. All reactions were carried out under 1 atmosphere of oxygen-free UHP-grade argon using standard Schlenck techniques or under a dry and oxygen-free nitrogen atmosphere using standard glovebox techniques. All solvents were dried and degassed by standard methods and distilled prior to use. The preparation of the starting materials $MM(TiPB)_4$ has been previously reported for MM = Mo_2,[58] MoW, and W_2.[31] The synthesis of the terthienyl carboxylic acid (TTh-H) was accomplished by following reported procedures,[59] and the synthesis of the compound $Mo_2(TiPB)_2(TTh)_2$ has also been reported.[29]

MoW(TiPB)$_2$(TTh)$_2$. MoW(TiPB)$_4$ (0.183 g, 0.144 mmol) was dissolved in 30 mL of dry toluene, and this yellow solution was canulated to a Schlenck flask containing TTh-H (0.08 g, 0.27 mmol). The suspension was stirred at room temperature for 4 days, at the end of which a blue precipitate had formed. This was centrifuged and washed with toluene (2 × 10 mL) before being dried in vacuo to give 160 mg (82% yield) of a blue solid. Microanalysis found: C 51.18, H 4.41 $C_{58}H_{60}O_8S_6MoW$ requires: C 51.33, H 4.46. NMR (THF-d_8): δ_H (400 MHz) 7.69 (d, 2H, J_{HH} = 4 Hz), 7.39 (d, 2H, J_{HH} = 4 Hz), 7.37 (d, 2H, J_{HH} = 5 Hz), 7.33 (d, 2H, J_{HH} = 4 Hz), 7.28 (d, 2H, J_{HH} = 4 Hz), 7.22 (d, 2H, J_{HH} = 4 Hz), 7.05 (dd, 2H, J_{HH} = 3.5 Hz), 7.02 (s, 2H), 3.03 (m, 4H), 2.88 (m, 2H), 1.24 (d, 12H, J_{HH} = 7 Hz), 1.12 (d, 24H, J_{HH} = 7 Hz) ppm. MALDI-TOF: Calculated monoisotopic mw for $C_{58}H_{60}O_8S_6MoW$: 1358.1. Found: 1359 (M^+). UV−vis−NIR (in THF, 293 K, values of ε are given in parentheses): 632 br (~37000), 379 (~81000) nm.

W$_2$(TiPB)$_2$(TTh)$_2$. $W_2(TiPB)_4$ (0.099 g, 0.073 mmol) was dissolved in 30 mL of dry toluene, and this yellow solution was canulated to a Schlenck flask containing TTh-H (0.041 g, 0.142 mmol). The suspension was stirred at room temperature for 4 days, at the end of which a green precipitate had formed. This was centrifuged and washed with toluene (2×10 mL) before being dried in vacuo to give 85 mg (81% yield) of a green solid. Microanalysis found: C 48.08, H 4.21 $C_{58}H_{60}O_8S_6W_2$ requires: C 48.20, H 4.18. NMR (THF-d_8): δ_H (400 MHz) 7.50 (d, 2H, J_{HH} = 4 Hz), 7.45 (d, 2H, J_{HH} = 4 Hz), 7.39 (dd, 2H, J_{HH} = 5 Hz), 7.30 (dd, 2H, J_{HH} = 4 Hz), 7.28 (d, 2H, J_{HH} = 4 Hz), 7.26 (d, 2H, J_{HH} = 4 Hz), 7.08 (dd, 2H, J_{HH} = 3.8 Hz), 7.07 (s, 2H), 2.97 (m, 4H), 2.90 (m, 2H), 1.27 (d, 12H, J_{HH} = 7 Hz), 1.13 (d, 24H, J_{HH} = 7 Hz) ppm. MALDI-TOF: Calculated monoisotopic mw for $C_{58}H_{60}O_8S_6W_2$: 1442.2. Found: 1445 (M^+). UV−vis−NIR (in THF, 293 K, values of ε are given in parentheses): 769 (~71000), 715 (~62000), 384 (~89000) nm.

Theoretical Approaches

Electronic structure calculations on the model compounds **I′**, **II′**, and **III′** were performed DFT with the aid of the Gaussian03 suite of programs. The B3LYPexchange correlation functional[60,61] was used along with the 6-31G* basis set for C, H, and O, 6-31+G (2d) basis set for S, and the SDD energy consistent pseudopotentials for molybdenum and tungsten. Geometry optimizations were performed in appropriate symmetry and were confirmed as local minima on the potential energy surfaces using frequency analysis. Orbital analyses were preformed using Gaussview.

Acknowledgment. We would like to thank the National Science Foundation and the Institute of Materials at Ohio State University for funding. We would also like to thank the Ohio Supercomputing Center for computing resources. We also thank Prof. Felix N. Castellano and Dr. Aaron Rachford at Bowling Green State University for assistance with emissive lifetime determinations of compound **III**.

Supporting Information Available: Listing of absorption, emission, and excitation spectra for the ligand TTh-H, solvatochromic studies on compound **III**, and ns TA spectrum of compound **I**. This material is available free of charge via the Internet at http://pubs.acs.org.

(57) Burdzinski, G.; Hackett, J. C.; Wang, J.; Gustafson, T. L.; Hadad, C. M.; Platz, M. S. *J. Am. Chem. Soc.* **2006**, *128*, 13402.
(58) Cotton, F. A.; Daniels, L. M.; Hillard, E. A.; Murillo, C. A. *Inorg. Chem.* **2002**, *41*, 1639.
(59) Wang, S.; Brisse, F. *Macromolecules* **1998**, *31*, 2265.
(60) Becke, A. D. *Phys. Rev. A: Gen. Phys.* **1988**, *38*, 3098.
(61) Miehlich, B.; Savin, A.; Stoll, H.; Preuss, H. *Chem. Phys. Lett.* **1989**, *157*, 200.